MACROSCOPIC ROTORS

ROGERS C. RITTER AND W. STEPHEN CHEUNG

DEPARTMENT OF PHYSICS, UNIVERSITY OF VIRGINIA
CHARLOTTESVILLE, VIRGINIA 22901 U.S.A.

in

Proceedings of the 1983 International School and Symposium on Precision Measurement and Gravity Experiment, Taipei, Republic of China, January 24 - February 2, 1983, ed. by W.-T. Ni (Published by National Tsing Hua University, Hsinchu, Taiwan, Republic of China, June, 1983)

445

OUTLINE

A. Macroscopic vs. Microscopic Rotors 447

B. Spherical vs. Axial Rotors 448

C. Axial Rotor Stability 449

D. Some Intrinsic Limits of a Rotor 452

E. Modes of An Axial Rotor 455

F. Practical Problems With A Precision Rotor 457

1. Fluctuation of measured rotor period.
2. Viscous drag of a rotor.
3. Bearing drag.
4. Thermal expansion.

G. Conclusions 462

References 463

MACROSCOPIC ROTORS*

Rogers C. Ritter and W. Stephen Cheung**

Department of Physics, University of Virginia
Charlottesville, VA 22901 U.S.A.

We have recently been carrying out developement on two gravitational experiments using ultra-precise macroscopic rotors.[1] These are: 1) a matter creation test in which the decay of rotational velocity would be an indication of matter increase in a rotor, and 2) a precision high-Q ($>10^{15}$) rotor forms the essential time base of an inertial clock, whose gravitational red-shift would differ from that measured by a hydrogen maser if gravity departs from the metricity of General Relativity. Other possible experiments come to mind if the intended rotor precision--including demonstrable decay time $\tau^* \sim 10^{18}$s--is achieved.

This paper discusses, first, a few simple fundamental relationships for assessing microscopic vs. macroscopic rotor properties, then some classifications, basic properties and limits of macroscopic rotors and finally some of the practical problems and research we have done with these rotors.

A. Macroscopic vs. microscopic rotors

The relationship between precision macroscopic and microscopic rotors has much the character of the principle of complementarity with respect to the nature of the observations. We assume solid-body rotors, so the collective motion of particles in a macroscopic rotor is, within limits, guaranteed and leads to high observability for a single rotor. This is unlike atomic, nuclear or molecular rotors, whose singular interrogation leaves virtually no rotational information. (It is, instead, the collection of information from many of these rotors that leads to the sought-for practical result.)

A beautiful property of a given atom or nucleus is that (we believe) it is exactly like every other one of its species. This is strictly true only for the "free" particle undisturbed by the presence of perturbing fields. Thus it is incumbent on a given atomic experiment to provide assurance that the collective effect measured is in fact representative of the species. Or, in cases where only constancy is of interest, the perturbations must be so uniform and constant that the intrinsic stability of the measured effect is retained to the level needed.

No two macroscopic rotors are expected to be as alike as two particles of a given kind. Nor are they as ideally symmetric (in whatever symmetry they do have). Thus a macroscopic rotor lacks a certain fundamental character inherent in, say, an atom. (It is, of course, only on faith that we believe in the absolute fundamentality of any type of particle thus far observed.) Nevertheless, particles seem, on the fact of it, to be more fundamental than macroscopic rotors.

Practically, the consequences of the above differences have to do much with the extreme differences in the nature and handling of their disturbances, as will become apparent.

Another practical matter is that atoms have frequencies 10^{15} greater (we consider macroscopic rotors with period $T_o \sim 1$ s). When doing measurements to a precision of 10^{15}, it is clear that atoms have, directly, the more useful information for timing things in a reasonable epoch. In fact, the timing of varying events with a macroscopic rotor to high precision is impossible unless an appropriate "time vernier" is found. Fortunately, the atomic experiments have already dealt with some of those methods. For example, the practical cesium-beam clock locks the relevant atomic oscillation to a crystal oscillator of much lower frequency.

Thus it seems that, at least in the present stage of development, atomic rotors have for many precision purposes, huge advantages. We, nevertheless, will present here studies of the macroscopic rotor in following sections. And, we also will keep in mind that for purposes of many conceptual gravitational experiments, the atomic rotor is not always the appropriate one.

B. Spherical vs. Axial Rotors

The type of rotor discussed here has cylindrical symmetry and has the axis constrained to a fixed direction. (This is only approximately true, as will be seen.) Spherical rotors have the disadvantage, for the above purposes, of precession of the body-fixed spin axis. Thus the measurement of angular velocity becomes more complex than it is for an axial rotor.

The means of constraint for a cylindrical rotor (meaning here a rotor having a single axis of rotational symmetry) are of interest. In the usual magnetically suspended rotor, whether spherical or not, there is a "vertical" axis maintained by gravity and the near absence of friction. The "vertical" axis force is in fact partly gravitational and partly inertial. The earth's rotation causes a constant turning of that axis if the rotor is suspended from a fixed point on the earth (except at the poles). The constancy of even that rotation, as well as of the magnitude of the attraction is not high on the scale of precision of interest here. All of these lead to the need for consideration of such geophysical effects and their correction in a true precision experiment.

The achievement of an axially-constrained rotation in a satellite experiment is a different matter, and is meaningless in the usual scheme of a magnetic suspension. Typically the reason for such a location of the experiment would be the establishment of near zero gravitational field, e.g. the Stanford Relativity Gyro experiment.[3] An external means is therefore in such cases needed for the reference frame with which the spin axis is to be measured (or constrained). In the Stanford experiment a telescope sighting on a "fixed star" provides that frame and the change of the gyro axis of the spinning sphere is the measurement of interest.

We restrict our interest here, however, to the scalar magnitude change of the spin angular velocity. Thus a sphere may not always be the best rotor for our purposes. For one thing, even the best spheres to date have lacked true geometric and mass sphericity beyond the 10^{-7} level. Beams[4] and Fremery[5] did use small magnetically suspended spheres for purposes such as we have in mind. These rotated usually at high speed, ~10^3 to 10^6 Hz, and developed oblateness about the spin axis which would be of consequence only in its constancy.

One problem of such spherical rotors is geophysically induced. The spin-spin coupling of the rotor to the earth yields a constant precession torque, termed[6] the "Keith Coriolis Torque". This causes a rotor to hang slightly toward one of the poles of the earth and thereby to generate a tiny eddy-current drag due to the non-colinearity of the true spin and magnetic support axes. (Eddy currents in a spinning magnetically suspended rotor align its spin axis with the support axis. If this were constant in inertial space there would be no such drag.)

It is surprising that, by careful analysis and by experiment[6], the Keith drag is barely ω- (angular velocity) dependent. Thus, larger, slower spherical rotors do not gain in this effect. It seemed advantageous to use larger, non-spherical rotors and Fig. 1 shows one we use. In this ~ 5% of the mass, at the top, is ferromagnetic and provides the support. The precession-caused hangofff in such a rotor becomes a much different matter than in the Keith calculation, and we have not yet studied it.

Such a rotor, having new symmetries, leads to new modes and their problems, as well as placing an added burden on suspension stability. Some of this will be discussed in following sections.

C. Axial rotor stability.

The stability of a free symmetric body has been well-studied.[7] We take up the also well-known special case of our axially symmetric rotor and use a relatively elementary analysis. The Euler equations of motion for a free symmetric rotor (i.e. having 3 principal axes of symmetry) are:

$$\Gamma_1 = I_1\dot{\omega}_1 + (I_3-I_2)\omega_2\omega_3 = 0,$$

$$\Gamma_2 = I_2\dot{\omega}_2 + (I_1-I_3)\omega_1\omega_3 = 0,$$

and

$$\Gamma_3 = I_3\dot{\omega}_3 + (I_2-I_1)\omega_2\omega_1 = 0, \qquad (1)$$

where Γ_1, Γ_2 and Γ_3 are torques about the three body axes (principal axes of inertia) and are set to zero, I_1 to I_3 are the corresponding moments of inertia, and ω_1 to ω_3 are the angular velocities.

We choose the 3 axis as the main spin axis, which also is the axis of symmetry, so that $I_1 = I_2$, or very nearly. Thus for perfect rotation,

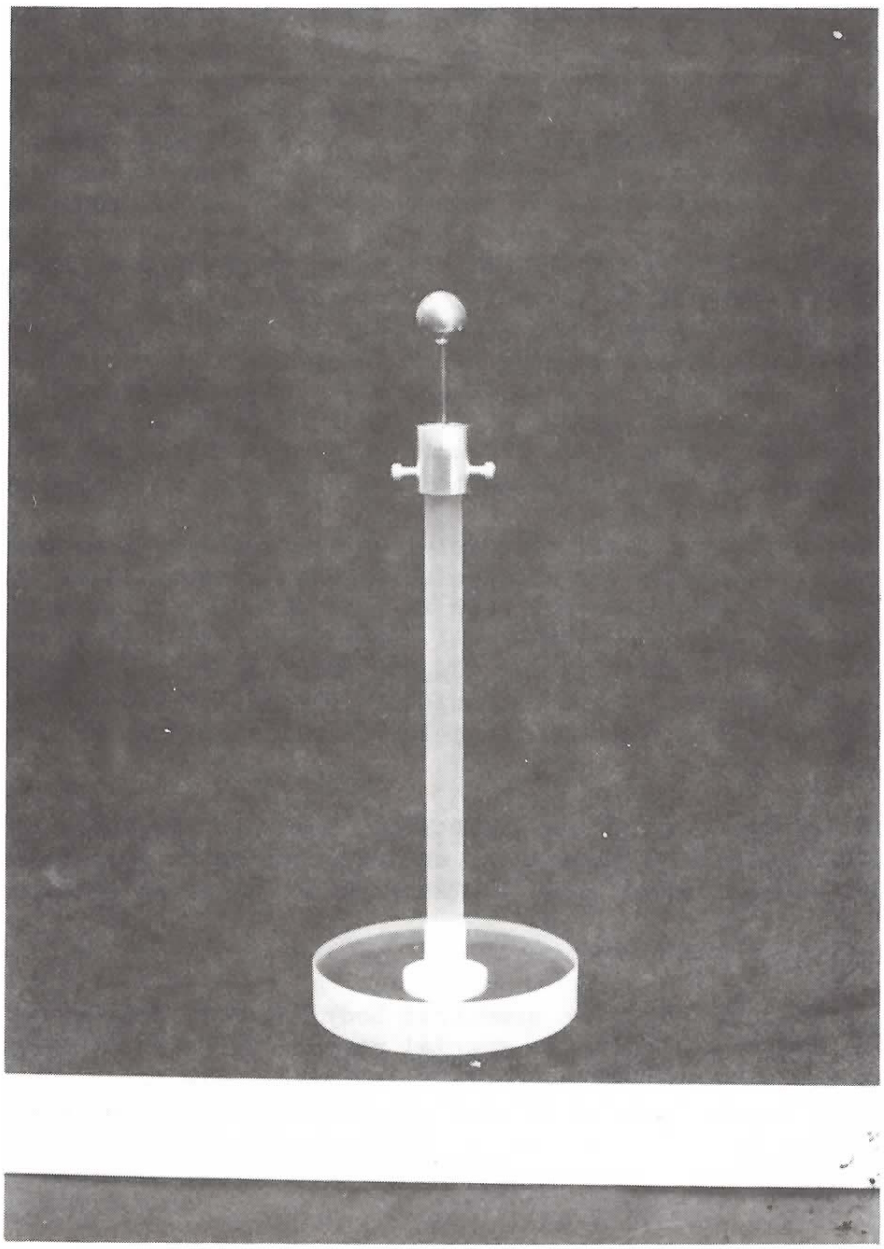

Fig. 1 Precision rotor for matter creation experiment. The disc at bottom and main shaft are of ultra-stable Zerodur. An aluminum collar and rod attach this to the annealed iron support sphere. A mirrored surface on the collar provides angular position sensing by means of a reflected laser beam.

$\omega_1=\omega_2=0$, and $\omega_3=\omega$. If there are perturbations, however, so that at some moment

$$\omega_3 = \omega + \xi,$$

$$\omega_1 = \eta,$$

and

$$\omega_2 \quad \zeta, \tag{2}$$

with ξ,η and ζ having small values $<<\omega$, we can evaluate conditions for which they lead to increase (instability) or limitation of the ξ, η and ζ.

From differentiation and rearrangement of (1) (with the Γ's set to zero) we have

$$I\ddot{\omega}_1 = (I_2-I_3)(\dot{\omega}_2\omega_3+\dot{\omega}_3\omega_2),$$

$$I_2\ddot{\omega}_2 = (I_3-I_1)(\dot{\omega}_3\omega_1+\dot{\omega}_1\omega_3),$$

and

$$I_3\ddot{\omega}_3 = (I_1-I_2)(\dot{\omega}_1\omega_2 + \dot{\omega}_2\omega_1), \tag{3}$$

where I_1 and I_2 are not yet made equal. Insertion from (1) leads to the form

$$\ddot{\omega}_i = [F(I)\omega_j^2 + G(I)\omega_k^2]\omega_i, \tag{4}$$

where i, j and k are permutations of 1, 2, 3 and F(I) and G(I) are of the form,

$$\left(\frac{I_i-I_j}{I_k}\right)\left(\frac{I_k-I_i}{I_j}\right),$$

and

$$\left(\frac{I_i-I_j}{I_k}\right)\left(\frac{I_j-I_k}{I_i}\right), \tag{5}$$

respectively.

If, in (4) the [ ] factor is positive, ω_i blows up. If it is negative, that ω_i oscillates.

If we now assume $I_1=I_2$ (4) becomes

$$\ddot{\omega}_3 = 0$$

$$\ddot{\omega}_1 = -\left(\frac{I_1-I_3}{I_1}\right)^2 \omega_3^2\omega_1,$$

and

$$\ddot{\omega}_2 = -\left(\frac{I_1-I_3}{I_3}\right)^2\omega_3^2\omega_2. \tag{6}$$

Inserting the perturbations (2) and assuming ω = constant we have.

$$\ddot{\xi} = 0$$

$$\ddot{\eta} = -\left(\frac{I_1-I_3}{I_1}\right)^2\omega^2\eta,$$

and

$$\ddot{\zeta} = -\left(\frac{I_1-I_3}{I_1}\right)^2\omega^2\zeta. \qquad (7)$$

The second and third of these always have negative coefficients of η,ζ on the r.h.s. and hence are oscillatory in these perturbations. If there is any damping in the system they will decay. ξ could grow linearly but would require continuing energy input. It can easily be shown that if I_1 is not exactly equal to I_2, the perturbations will still be oscillatory whether $I_3 < I_1, I_2$ or the reverse.

Thus there is not a tendency of instability in the free axially symmetric rotor except for the nearly spherical case. In the constrained rotor this would be worst for I_3 intermediate between I_1 and I_2, as is well known. In our rotors, however, we have totally avoided this possibility. A long shaft, as shown in Fig. 1, is used for other reasons[8], but also accomplishes this.

D. Some intrinsic limits of a rotor

In this section we further limit our discussion to rotors of a few cm diameter and having $0.1 < \omega < 10$ rad/s. Reasons for such limitations in our research have been discussed.[8,9] The periods of these rotors are measured and the constancy of the periods against fluctuation and decay are of primary interest.

The intrinsic limits of interest here for such a rotor are from thermal fluctuations and fluctuations and decay caused by light-beam sensing of the rotor period.

The differential equation for the rotational motion of an unfedback rotor is

$$I\ddot{\theta} + \kappa\dot{\theta} + c\theta = \Gamma(t), \qquad (8)$$

where I is the moment of inertia, κ the drag coefficient, c a torsional coupling, and $\Gamma(t)$ an applied torque, for example noise. In the successful rotor c will be significantly near zero as will $\Gamma(t)$. Thus the decay time for free rotation will be

$$\tau^* = \omega/\mathring{\omega} = I/\kappa, \qquad (9)$$

where $\omega = \mathring{\theta}$.

In addition to decay from frictional mechanisms leading to κ, there are thermal fluctuations which lead to a random walk about the position predicted from the decay equation. For a system with some couple these are found from consideration of the mean potential energy

of this system of one degree of freedom,

$$\frac{1}{2}c\overline{\Delta\theta_n^2} = \frac{1}{2}kT, \tag{10}$$

where $\Delta\theta_n$ is the rms thermal fluctuation of angle, k is Bolzman's constant and T the temperature.

If, however, the suspension is torsionless, this is replaced by[10],

$$\frac{1}{2}I\overline{\Delta\omega_n^2} = \frac{1}{2}kT, \tag{11}$$

where $\Delta\omega_n$ is the rms fluctuation of velocity. McCombie[10] evaluates this two ways, leading to,

$$\overline{\Delta\theta_n^2} = 2kT/\kappa\ [\Delta t - \tau^*\{1-\exp(-\Delta t/\tau^*)\}], \tag{12}$$

where Δt is the observation time during which the rotor has departed by $\Delta\theta_n$. In all of our experiments $\Delta t << \tau^*$, so that

$$\overline{\Delta\theta_n^2} \approx (kT/I)\Delta t^2. \tag{13}$$

At room temperature and for I $\approx$ 2000 gm-cm^2, the factor (kT/I) is about 10^{-18} (rad/s)^2.

Our measurement is always the period or period fluctuation.[11] Thus the angle random walk is effectively an angular velocity fluctuation which varies the time of each period by an amount

$$\Delta T_r = (T_o/2\pi)\Delta\theta_n, \tag{14}$$

where T_o is the mean period. For single period fluctuation estimates $\Delta\theta_n$ would be the fluctuation during $\Delta t = T_o$. However, the great advantages of rotors in precision are their ability to be averaged over many periods to decrease the measurement error. Thus in general we average over N periods, where N = 1, 10, 100, 1,000 or 10,000. In this case $\Delta t = NT_o$ and $\Delta\theta_n$ becomes the random walk in N periods: Thus

$$\Delta T_r(N) = (T_o/2\pi)(kT/I)^{1/2}\ \Delta t, \tag{15}$$

and

$$\Delta T_r(N) = (1/2\pi)(kT/I)^{1/2}NT_o^2. \tag{16}$$

If we define the characteristic rotor fluctuation time $(kT/I)^{-1/2}$ as τ_r this takes the form

$$\Delta T_r(N) = [T_o^2/(2\pi\tau_r)]N. \tag{17}$$

$\Delta T_r(N)$ is linear with N and quadratic with T_o. It is convenient to use a normalized fluctuation

$$\Delta T_r(N)/T_o = [T_o/2\pi\tau_r)]N, \tag{18}$$

which is linear with T_o.

In addition to thermal fluctuation of the rotor there are effects caused by observation of the rotor with a light beam.[1] These include fluctuation from photon statistics and torques of a continuous nature.

The fluctuations arising from statistics are dependent on the mechanism of the photon sensor of rotor period. We use a small spot of laser light reflected from a mirrored surface. For a perfect mirror there would be no tangential momentum transfer by the photons to the rotor and hence no rotor fluctuation from the fluctuating photon density asymmetry. In fact there is some absorption, ~ 1% and such an effect does occur. The magnitude is much less than other fluctuations however, and can be ignored when compared with the rotor timing observation error.[1,12]

A steady beam of light on a rotor causes at least two continuous torques. Misalignment of direction from the rotation axis causes an obvious, but not intrinsic, torque caused by tangential momentum transfer of the partially absorbed beam. An intrinsic effect, however, has been studied by Braginsky[12] and is termed the "rotational ponderomotive instability". This results in a driving torque which tends to speed up the rotor.

The ponderomotive instability arises when a uniform beam causes differential heating. The part of the rotor arriving in the beam will be cooler, having just come from the shadow. A differential thermal coefficient of absorption, $\alpha = d\theta/dT$ where θ is the mean value of the coefficient of absorption, leads to a variable photon absorption across the part of the rotor struck by the beam and hence a torque.

This effect has been calculated and measured for a hollow rotating cylinder.[12] The change in angular velocity over a time Δt is

$$\Delta\omega \approx \frac{\omega_o{}^2 a^*}{(\lambda_{11}{}^2 \kappa)^2}, \tag{19}$$

where

$$a^* = \frac{a_1}{2\pi\kappa\lambda_{11}{}^2}. \tag{20}$$

Here λ_{11} is related to an eigenvalue of a hollow cylinder, κ is the coefficient of thermal conductivity and a_1 is a function of the beam intensity and some geometrical factors. For a small cylinder of 1 cm radius, 1.5 cm height and 15 μm thick a speed increase of about 3% was observed in 1800 s, in agreement with these equations.

E. Modes of an axial rotor.

A rotor such as that of Fig. 1 is suspended magnetically at the top by a force that can be approximated as a critically damped spring in the vertical direction. As such it has a sufficient number of degrees of freedom to develope some complex modes of motion.

Modes involving coupling to the vertical spring mode are not taken up here. In long runs, the high damping of this mode, and low damping of others, combined with the higher frequency (typically 20-75 Hz) of the vertical oscillation mode, render it less important. We note, however, that observation of this vertical motion by spectral analysis (with a Hewlett Packard Model HP-3582A Analyzer) allows study of some of the other motion.

The length of the bob of this rotor, viewed as a pendulum, gives a "pendulum frequency" of 1.10 Hz which is seen in the spectrum whenever the rotor is disturbed. In fact, the motion is a combination of the axial rotor rotation and conical pendulum motion. This is a particular case of the spinning (inverted) top.

Fig. 2 depicts the symmetric top.[13] Here x, y and z is the cartesian laboratory frame and the 1, 2, 3 axes are the body-fixed axes for rotation about the 3 axis. θ, ϕ, and ψ give the polar, precession and spin angles of the rotor. Clearly θ is very near π.

The standard derivation[7,13], leads to a 'potential energy' 'V'(θ) with an associated 'torque'

$$'\Gamma' = -\frac{\partial' V'}{\partial\theta} = mg\ell\sin\theta - \frac{(p_\phi - p_\psi\cos\theta)(p_\psi - p_\phi\cos\theta)}{I_1\sin^3\theta}, \tag{21}$$

where p_ϕ and p_ψ are appropriate angular momenta. Notice that 'Γ' is negative for $\theta \approx \pi$.

For pure precession at polar angle θ_o,

$$\dot{\phi}_o = \frac{p_\phi - p_\psi\cos\theta_o}{I_1\sin^2\theta_o} = \frac{I_3\omega_3}{2I_1\cos\theta_o}\left[1 \pm (1-2\alpha\cos\theta_o)^{1/2}\right], \tag{22}$$

where

$$\alpha = \frac{2mg\ell I_1}{I_3^2\omega_3^3}. \tag{23}$$

Since $I_1 \approx m\ell^2$ and $I_3 \approx 1/2\ mR^2$, where R is the radius of the disc of the rotor, this is approximately

$$\alpha \approx \frac{8g\ell^3}{R^4\omega_3^3}, \tag{24}$$

and

$$\dot{\phi}_o \approx \frac{1}{4}\left(\frac{R}{\ell}\right)^3 \frac{\omega_3}{\cos\theta_o}\left[1 \pm (1-2\alpha\cos\theta_o)^{1/2}\right]. \tag{25}$$

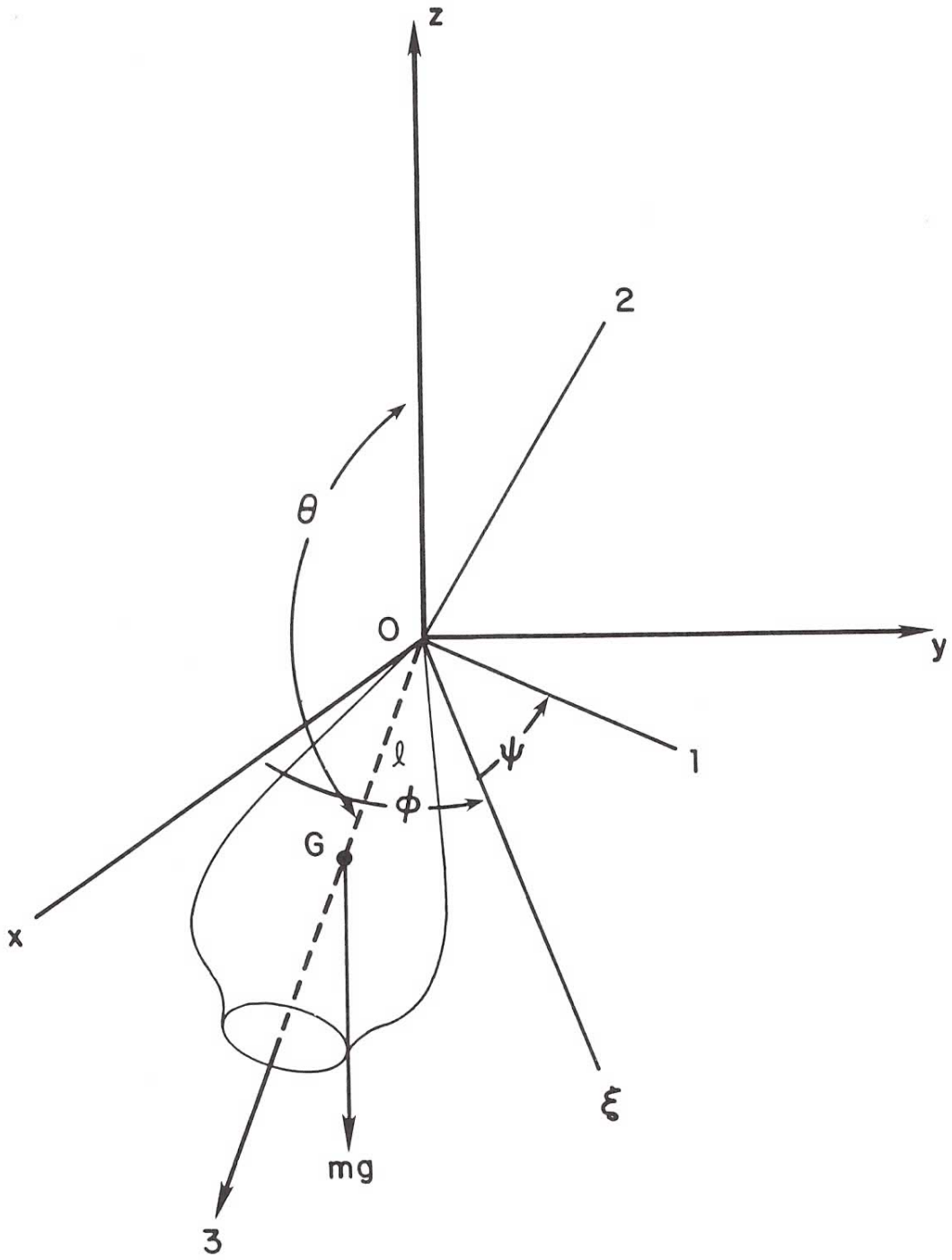

Fig. 2 Coordinates for the symmetric top.

Finally, for $\theta_o \approx \pi$,

$$\dot{\phi}_o(\pi) \approx -\frac{1}{4}\left(\frac{R}{\ell}\right)^2 \omega_3[1 \pm (1+2\alpha)^{1/2}]. \tag{26}$$

This can be manipulated further,

$$\frac{\dot{\phi}_o(\pi)}{\omega_3} = [-\frac{1}{2}I_3/I_1 \mp 2\frac{\omega_p}{\omega_3}], \tag{27}$$

where $\omega_p^2 = g/\ell$ is the pendulum frequency.

For the rotor of Fig. 1 $I_3/I_1 \approx 1/2(R/\ell)^2 = 0.01758$. We have made several mode tests for rotor periods of 3 and 4s, for which $\omega_3 = 2\pi/3$ and $2\pi/4$, respectively. Since ω_p is observed (or calculated) to be 6.9 rad/s, these lead to $\omega_p/\omega_3 = 3.3$ and 4.4, respectively.

Eq. (27) yields nearly degenerate antisymmetric solutions, with a difference for ϕ_o of $1/2\ (I_3/I_1)\omega_3 = 0.0088\omega_3$, or 0.0184 and 0.0138 rad/s for the two values of ω_3 tested. We might expect to observe a modal energy exchange between pure rotation and maximum "coning" with periods of 5.7 and 7.6 min., respectively. What are observed are such exchanges with periods of (2.55 ± 0.13) and (4.1 ± 0.2) min. for the rotor periods of 3s and 4s, respectively. This is highly repeatable and the departure from the calculated values is not understood, although the approximations for I_1, I_3 are not very good.

F. Practical problems with a precision rotor

Years ago Beams[14] listed 15 factors which might lead to deceleration of a rotor. A newer, somewhat modified list is given in ref. 11. We have studied a number of these and will present several of them, along with other factors which lead to imprecision of measured rotor periods.

1. Fluctuation of measured rotor period.

In addition to the intrinsic thermal fluctuation of a rotor, discussed in Section D, there is at least one more factor contributing error to the measured period.[11] This is the intrinsic instrumental error, ΔT_o. Since it is presumably an independent error, it can be added in quadrature to the thermal fluctuation ΔT_r of eq. (16),

$$\Delta T = \sqrt{\Delta T_o^2 + \Delta T_r^2}\ . \tag{28}$$

This applies to different measuring times, i.e. different numbers of periods averaged per data point.

For the range of periods used in our experiments the instrumental timing error, ΔT_o, is only slightly dependent on period. It is therefore a suitable approximation to assume that $\Delta T_{ON} = \Delta T_{01}/N$ gives the fluctuation in time of N periods by this mechanism, when ΔT_{01} is that for one period. Using this and the expression for ΔT_r from eq. (17) in eq. (28) we have,

$$\Delta T = \sqrt{\Delta T_{01}^2/N^2+(T^4/\tau_r^2)N^2}. \quad (29)$$

Asymptotically, for N small this has a slope of -1 on a log-log plot of ΔT vs N, or vs Δt. For N large it has a slope of +1. Typically for us $\Delta T_{01} \sim 1\text{-}2\times10^{-7}$s and $\tau_r \sim 10^8$s, so that for N=1 we determine ΔT_{01} and for $N = 10^3$ or 10^4 we estimate an effective value for τ_r, or correspondingly an effective temperature.

It is difficult to gather a sufficient ensemble of data for $N = 10^3$ or 10^4 because of the length of undisturbed runs needed. We have made a few dozen such runs for $N=10^3$ and several for 10^4. Unfortunately for $N=10^4$ the straight line decay approximation to $e^{-\Delta t/\tau^*}$ is no longer valid. This combines with the spectral filtering inherent in such large averaging to make it difficult to evaluate ΔT_r as fluctuations about a known exponential decay line for a span of points of small size given in a week or less of undisturbed running time. Consequently we have not yet made good asymptotic estimates of ΔT_r although the trend is readily apparent.

In data and analysis presented in ref. 11 we believed that the +1 asymptotic slope was demonstrated from the pattern of many runs even though single runs were not precise enough for reasons given above. Since then we have made improvements in data taking and in stability and have found reason to reinvestigate the earlier data. In the process we found a conceptual mistake in our data handling which had the effect of dividing each measured value of ΔT by N. A rework of this data and addition of a new set of careful measurements leads to the strong possibility that the asymptotic slope for large N is +2, not +1 as formerly believed and as given by eq. (29). This leads to the question of whether 1/f noise could be present and add to the slope, by +1. Further study is clearly needed.

2. Viscous drag of a rotor.

It has long been known[4] that a spinning rotor acts as a pressure gauge. In the free molecule regime it seems likely to provide an absolute standard of pressure measurement, and a commercial instrument of this type is now available. An outline of the derivation of the gas drag on a rotor[15] is the following.

From kinetic theory in the free molecule regime the momentum exchange leads to a force per unit area of

$$\frac{dF}{dA} = -\ 3/4\ \mu P\ \left(\frac{\bar{v}}{v^2}\right), \quad (30)$$

where μ is the velocity of the wall relative to the gas. (This point is very important in the use of corotation of the gas as a means of reducing drag.) Also, P is the pressure and $\bar{v}$ the average speed of the molecules. For a Maxwell velocity distribution

$$\frac{\bar{\nu}}{\nu^2} = \frac{4}{3}\left(\frac{m}{2\pi kT}\right)^{1/2}, \tag{31}$$

where m is the mass of the molecule and k and T are as before. Hence

$$\frac{dF}{dA} = -\mu P\sqrt{\frac{m}{2\pi kT}} = -\mu Z, \tag{32}$$

where $Z = P\sqrt{m/2\pi kT}$.

The decelerating torque per unit area of a thin cylinder of radius r and angular velocity ω is

$$\frac{d\Gamma}{dA} = -\omega r^2 z, \tag{33}$$

or the total torque is

$$\Gamma = -\omega Z \int_s r^2 dA \tag{34}$$

where the surface integral is over the rotating surface.

Often solid rotors of density ρ are used, in which case the moment of inertia is

$$I = \rho \int_v r^2 dV. \tag{35}$$

For an exponentially decelerating rotor of decay time τ^*,

$$\omega = \omega_o e^{-t/\tau^*}, \tag{36}$$

and hence

$$\frac{\dot{\omega}}{\omega} = -\frac{1}{\tau^*}. \tag{37}$$

Finally, we have

$$\tau^* = \frac{\rho}{Z}\,\frac{\int_V r^2 dV}{\int_A r^2 dA}. \tag{38}$$

This can be evaluated for a cylinder of height h and radius a:

$$\tau^* = \frac{\rho a}{2Z(2+ a/h)}, \tag{39}$$

and for a sphere of radius a:

$$\tau^* = \frac{\rho a}{5Z}. \tag{40}$$

In the early literature[4] the factor C appeared in the denominator of (39) and (40). Taking a value from 1 to 2, it was used to handle

the "accomodation coefficient" related to the behavior of colliding molecules at the surface. With appropriate materials and procedure it can be made very nearly unity.

Since Z is proportional to P, it is to be seen that τ^*P = const. for a given cylindrical or spherical rotor. For the rotor of Fig. 1,

$$\tau^* = 59/P, \tag{41}$$

if the Pressure P is in Torr, so that at 10^{-6} torr, the gas drag time constant is about 6×10^7s.

3. Bearing drag.

In section B the geophysically-incuded eddy current bearing drag was discussed. It presumably could be removed by the use of a superconducting bearing, in which the earth would induce other responses but eddy current loss would not be present.

In the ferromagnetic suspension, however, the "Keith Coriolis" torque led to limit of $\tau^* \sim 10^{10}$s in tests by Beams and Fremery. In practice, we usually find τ^* much lower[11,16]. Our lower speed rotors of lower symmetry and greater force per unit suspension material volume would be expected to emphasize anomalous eddy current effects.

We have studied these[16,18] and found a strong rotational frequency dependence of τ^*. In the studies we discovered a parametric pumping effect whereby the rotor had energy pumped into or out of its rotational motion by the suspension. This comes about in the following way. As the rotor spins, it bounces synchronously. This is due to anomalous light reaching the optical suspension detector in varying amounts as it spins, causing a false sense and reaction in the servo. The amount of bounce in a non-corotation rotor is about 10 μm or less, but sufficient to couple into azimuthal asymmetries of the suspension potential and parametrically exchange energy.

Very recently we have discovered a strong correlation between the rotational speed and the suspension resonance. The harmonics of the rotor frequency appear, up to the 8th or higher, in the suspension sensor signal. When the 6th or 8th harmonic lies sufficiently near the suspension resonance peak a dip appears in the decay time spectrum.[16,17]

We have found a way to evaluate bearing and gas drags independently.[17] This assumes that gas drag is proportional to relative angular velocity. In our corotation apparatus we vary the direction and angular velocity of the gas surrounding a spinning rotor. With the appropriate differential equation and definition of relative periods, the data leads to a straight line whose slope and intercept give the relevant information. In particular, we have learned that an excess bearing drag occurs when the corotation is synchronous or counter-synchronous (same speed but opposite direction). The added bounce at these conditions presumably contributes more to the energy exchange.

4. Thermal expansion.

Thermal changes in a rotor give radius variations which lead to angular velocity drifts that can mask the sought-for information. For this reason our rotor discs (7.5 cm diameter for the rotor in Fig. 1) are of the most stable material possible, an optical glass-ceramic: Zerodur. This has a linear expansion coefficient $\alpha = 5 \times 10^{-8}$ per °C for the best grade at room temperature.

From conservation of angular momentum

$$L = I\omega, \tag{42}$$

we find

$$\frac{d\omega}{\omega} = - \frac{dI}{I} = - 2 \frac{dr}{r}, \tag{43}$$

if $I = 1/2\ mr^2$ and m is constant. The expansion coefficient α gives

$$\frac{dr}{r} = \alpha dT, \tag{44}$$

for a differential temperature change dT, so that, with (43),

$$\frac{d\omega}{\omega} = -2\alpha dT. \tag{45}$$

In our matter creation experiment[1], a change of moment of inertia $\dot{I}/I$ of 10^{-10} per year would lead to a $d\omega$ and be the signal of interest. A thermal temperature change which would mimic this is obtained from

$$\frac{dm}{m} = 2 \frac{dr}{r} = 2\alpha dT, \tag{46}$$

or

$$dT = \frac{dm/m}{2\alpha} . \tag{47}$$

Assuming $\dot{m}/m = \dot{I}/I$, then

$$\frac{dT}{dt} = \frac{\dot{m}/m}{2\alpha} = \frac{10^{-10}}{10^{-7}} = 1\text{mK/yr}. \tag{48}$$

Such a stringent limit can almost certainly not be reached at room temperature with the above value for α. It therefore provides another reason for doing the most precise rotor experiments at liquid helium temperature.

Alternatively, we can calculate what decay time is mimiced by a given temperature change. From (43) and (45) we can get

$$\frac{1}{\tau*} = - \frac{\dot{\omega}}{\omega} = \frac{\dot{I}}{I} = \frac{\dot{m}}{m} = 2\alpha \frac{dT}{dt}, \tag{49}$$

or

$$\frac{dT}{dt} = \frac{1}{2\alpha\tau^*} \quad . \tag{50}$$

For τ^* a modest 10^{10}s and the above α this required $dT/dt \leq 10^{-3}$ °C/s. On long runs such as those described for measuring fluctuations in Section D thermal variation can be a factor in this way.

G. Conclusions

Macroscopic rotors, though of lower apparent fundamentality than elementary particles or atoms, have potential as ultra-stable oscillators and also in other types of gravitational experiments. Their fluctuations and other precision-related properties have not been well-studied. Instrinsic limits of these aspects as well as a number of practical problems such as thermal effects are now the object of experimentation. Interesting and unanticipated features have appeared. As yet, no insurmountable problems have indicated a limit to the developement of precision rotors for gravitation experiments.

*Supported in part by NSF Grant PHY80-07948 and NBS Grant G8-9025.

**Present address: Hanson Laboratories, Stanford University, Palo Alto, CA 94305 (USA)

References

1. Rogers C. Ritter, in Proceedings of the Second Marcel Grossman Meeting Conference on General Relativity, Celebrating the 100th Anniversary of Einstein's Birth, Trieste, Italy, July 1979, ed. R. Ruffini (North Holland, Amsterdam, New York, Oxford, 1982) pp. 1039-1070.

2. Kurt Lambeck, The Earth's Variable Rotation (Cambridge Univ. Press, Cambridge, 1980).

3. J. T. Anderson, et al., in Proceedings of the Second Marcel Grossman Meeting on General Relativity, ed. Remo Ruffini, (North-Holland, Amsterdam, 1982) p. 939.

4. J. W. Beams, D. M. Spitzer and J. P. Wade, Rev. Sci. Instrum. 33, 151 (1962).

5. J. K. Fremery, Phys. Rev. Lett. 30, 753 (1973).

6. J. C. Keith, J. Res. Nat. Bur. Stand. 670, 533 (1963); J. K. Fremery, Rev. Sci. Instrum. 43, 1413 (1972).

7. See, e.g. Herbert Goldstein, Classical Mechanics, (Addison-Wesley, Reading, Mass., 1953).

8. G. T. Gillies, Dissertation, Univ. of Virginia, 1980, University Microfilms, Ann Arbor, Mich.

9. G. R. Jones, Dissertation, Univ. of Virginia, 1983, University Microfilms, Ann Arbor, Mich.

10. C. W. McCombie, Rept. Prog. in Phys. 16, 266 (1953).

11. George R. Jones, R. C. Ritter and George Thomas Gillies, Metrologia 18, 209 (1982).

12. V. B. Braginsky and A. B. Manukin, Measurements of Weak Forces in Physics Experiments, (Univ. of Chicago Press, Chicago, 1977).

13. Keith R. Symon, Mechanics, 3rd ed. (Addison-Wesley, Reading, Mass., 1971), p. 454.

14. J. W. Beams, Rev. Sci. Instrum. 34, 1071 (1963).

15. Wah-Kwan Stephen Cheung, Dissertation, Univ. of Virginia, 1982, University Microfilms, Ann Arbor, Mich.

16. George R. Jones, M. Sc. Thesis, Univ. of Virginia, 1981.

17. George R. Jones, George T. Gillies and Rogers C. Ritter, Prec. Engrg. 4, 79 (1982).